Proceedings of OMAE08
27th International Conference on Offshore Mechanics and Arctic Engineering
June 15-20, 2008, Estoril, Portugal

OMAE2008-57855

ON THE MODELING OF NONLINEAR WAVES FOR PREDICTION OF LONG-TERM OFFSHORE WIND TURBINE LOADS

P. Agarwal
Dept. of Civil, Arch., and Env. Engineering
University of Texas
Austin, TX 78712, USA
Email: pagarwal@mail.utexas.edu

L. Manuel*
Dept. of Civil, Arch., and Env. Engineering
University of Texas
Austin, TX 78712, USA
Email: lmanuel@mail.utexas.edu

ABSTRACT

In the design of wind turbines—onshore or offshore—the prediction of extreme loads associated with a target return period requires statistical extrapolation from available loads data. The data required for such extrapolation are obtained by stochastic time-domain simulation of the inflow turbulence, the incident waves, and the turbine response. Prediction of accurate loads depends on assumptions made in the simulation models employed. While for the wind, inflow turbulence models are relatively well established, for wave input, the current practice is to model irregular (random) waves using a linear wave theory. Such a wave model does not adequately represent waves in shallow waters where most offshore wind turbines are being sited. As an alternative to this less realistic wave model, the present study investigates the use of irregular nonlinear (second-order) waves for estimating loads on an offshore wind turbine, with a focus on the fore-aft tower bending moment at the mudline. We use a 5MW utility-scale wind turbine model for the simulations. Using, first, simpler linear irregular wave modeling assumptions, we establish long-term loads and identify governing environmental conditions (i.e., the wind speed and wave height) that are associated with the 20-year return period load derived using the inverse first-order reliability method. We present the nonlinear irregular wave model next and incorporate it into an integrated wind-wave-response simulation analysis program for offshore wind turbines. We compute turbine loads for the governing environmental conditions identified with the linear model and also for an extreme environmental state. We show that computed loads are generally larger with the nonlinear wave modeling assumptions; this establishes the importance of using such refined nonlinear wave models in stochastic simulation of the response of offshore wind turbines.

INTRODUCTION

While addressing different load cases, wind turbine designers are required to estimate extreme and fatigue loads; this is usually done by carrying out stochastic turbine response time-domain simulations. Simulation of an offshore wind turbine response involves simulations of the stochastic inflow wind field on the rotor plane and of the irregular (random) waves on the support structure. Once the wind and waves are simulated, the response of the turbine is computed in the time domain using an ceroplastic model of the turbine. Obtaining realistic response of the turbine depends, among other factors, on appropriate modeling of the incident wind and waves. The current practice for modeling waves on offshore wind turbines is limited to the representation of linear irregular waves. While such models are appropriate for deep waters, they do not offer accurate representations of waves in shallow waters where offshore wind turbines are most commonly sited. In shallow waters, waves are generally nonlinear in nature. It is, therefore, of interest to assess the influence of alternative wave models on the behavior of wind turbines (e.g., on the tower response) as well as on extrapolated long-term turbine loads. The expectation is that nonlinear (second-order) irregular waves [1] can better describe waves in shallow waters. In this study, we investigate differences in turbine response statistics and in long-term load predictions that arise from the use of alternative wave models.

The prediction of extreme loads for long return periods (on the order of 20-50 years, typically), as is required when address-

*Corresponding Author

ing at least one of the design load cases specified in the International Electrotechnical Commission (IEC) guidelines [2], relies on extrapolation of load statistics from a limited number of simulations. Extrapolation refers to estimation or prediction of a rare load fractile associated with the desired long return period. Several extrapolation techniques, such as direct integration of short-term load distributions (conditional on environmental conditions) appropriately weighted by the likelihood of occurrence of those conditions, as well as more efficient techniques such as the inverse first-order reliability method (inverse FORM) have been explored in wind turbine applications [3]. While extrapolated load estimates are known to be affected by statistical uncertainty, model uncertainty due to imperfect or unrealistic simulation models used can also result in errors in long-term load predictions. In this study, we will directly address the influence of model uncertainty as it pertains to modeling of waves. We will focus on how the sea surface elevation process, the water particle kinematics and, in particular, the hydrodynamic loads derived using a second-order nonlinear wave theory vary when nonlinear second-order waves are modeled as alternatives to the conventional linear first-order approach. We wish to note here that we will not address breaking of waves (which is generally thought to be important) since our focus is on long-term probabilistic load prediction by simulation and there is no well-established way to model irregular breaking waves.

We use a utility-scale 5MW offshore wind turbine model developed at the National Renewable Energy Laboratory (NREL) [4] in our simulation studies. The turbine is assumed to be sited in 20 meters of water. Stochastic time-domain simulations of the turbine response are performed using the computer program, FAST [5]. We first discuss the short-term response of the wind turbine to linear irregular waves; this represents existing capability of the offshore wind turbine response calculation in FAST (with respect to modeling of waves). We focus only on tower loads here (specifically, on the fore-aft tower bending moment at the mudline) since the influence of waves on loads on the rotor is not significant, as has been demonstrated in other studies (see, for example, Agarwal and Manuel [6]). We briefly discuss the procedure for extrapolated long-term load prediction using the inverse FORM technique. We then present the theory related to the development of a second-order nonlinear irregular wave model for simulation. For a coupled hydrodynamic and aeroelastic analysis of offshore wind turbines, we incorporate the nonlinear wave model in the computer program, FAST, for turbine simulations. We discuss how use of the nonlinear wave model can result in different (usually larger) loads on the support structure (a cylinder of 6 m diameter) of our 5MW turbine. We discuss the mechanics of loads due to nonlinear waves in detail and identify those circumstances where modeling nonlinear waves to derive realistic hydrodynamic loads may be most significant.

LOAD EXTRAPOLATION

Design Load Case 1.1b of the IEC 61400-3 draft design guidelines [2] recommends the use of statistical extrapolation to predict rare extreme turbine loads. Direct integration and the inverse FORM procedure are two common extrapolation methods. We have shown in an earlier study [6] that inverse FORM is as accurate as the direct integration method. We only use inverse FORM in the present study; this is discussed briefly next.

Direct Integration Method

In direct integration, one estimates the turbine nominal load for design, l_T, associated with an acceptable probability of exceedance, P_T, or, equivalently, with a target return period of T years, as follows:

$$P_T = P[L > l_T] = \int_{\boldsymbol{X}} P[L > l_T | \boldsymbol{X} = \boldsymbol{x}] f_{\boldsymbol{X}}(\boldsymbol{x}) d\boldsymbol{x} \qquad (1)$$

where $f_{\boldsymbol{X}}(\boldsymbol{x})$ represents the joint probability density function of the environmental random variables, $\boldsymbol{X}$ and L represents the load measure of interest. For different trial values of the load, l_T, Eq. 1 enables one to compute the long-term probability by integrating the short-term load exceedance probability conditional on $\boldsymbol{X}$, i.e., $P[L > l_T | \boldsymbol{X} = \boldsymbol{x}]$, with the relative likelihood of different values of $\boldsymbol{X}$. This method, while exact, is expensive as one is required to integrate over the entire domain of all the environmental random variables. In this study, two environmental random variables comprise $\boldsymbol{X}$; these are the ten-minute average wind speed, V, at hub height in the along-wind direction and the significant wave height, H_s, for waves assumed to be aligned with the wind.

Inverse FORM

Another extrapolation technique is the so-called inverse first-order reliability method (inverse FORM) [7]. Here, for the present application, one considers a surface in a three-dimensional space on one side of which (i.e., the "failure" side), it is assumed that $L > l_T$. The three dimensions of this space represent the jointly distributed variables, V, H_s, and L, and it is possible to mathematically transform this space to an independent standard normal space $\boldsymbol{U} = (U_1, U_2, U_3)$. A sphere of radius, β, in this space is defined as follows:

$$u_1^2 + u_2^2 + u_3^2 = \beta^2 \qquad (2)$$

This sphere is such that all values of $\boldsymbol{U}$ within it occur with a probability greater than P_T while all values outside it occurs with a probability less than P_T.

It is noted here that β is directly related to the target probability of load exceedance; namely, $P_T = \Phi(-\beta)$, where $\Phi()$ represents the cumulative distribution function of a standard normal random variable. The transformation of the random variables

involved from the physical $\boldsymbol{X}$ space to the standard normal $\boldsymbol{U}$ space is carried out via the Rosenblatt transformation such that $F_V(v) = \Phi(u_1)$, $F_{H|V}(h) = \Phi(u_2)$, and $F_{L|V,H}(l) = \Phi(u_3)$, where $F()$ denotes the cumulative distribution function in each case. A point on the sphere defined by Eq. 2 where the load attains its maximum value is the "design" point, and this load represents the desired nominal T-year return period load, l_T. Possible differences between this long-term load estimate and one obtained using direct integration per Eq. 1 result only due to an assumed linearization of the associated limit state function (for this failure mode) in the inverse FORM approach; however, this linearization approximation is not very inaccurate for rare loads associated with very small target probabilities of exceedance. The reader is referred to other studies (e.g., Saranyasoontorn and Manuel [3]) for details on the inverse FORM approach applied to derive long-term wind turbine loads.

Both the extrapolation methods discussed above require data on load extremes, which must be obtained from turbine simulations. Any limitations or approximations inherent in a simulation model can influence the accuracy of long-term load predictions. One such model approximation in simulations is introduced by way of the conventional use of a linear theory to model the waves. In the following, we discuss the influence of nonlinear irregular waves on simulated turbine tower loads, and how it can affect extrapolated long-term loads.

SIMULATION WITH LINEAR IRREGULAR WAVES

Simulation Model

A 5MW wind turbine model developed at NREL [4] closely representing utility-scale offshore wind turbines being manufactured today is considered here. The turbine is a variable-speed, collective pitch-controlled machine with a maximum rotor speed of 12.1 rpm; its rated wind speed is 11.5 m/s. It is assumed to have a hub height of 90 meters above the mean sea level, and a rotor diameter of 126 meters. It is assumed to be sited in 20 meters of water; it has a monopile support structure of 6 m diameter, which is assumed to be rigidly connected at the mudline. The turbine is assumed to be installed at an IEC Class I-B wind regime site [2]. A Kaimal power spectrum and an exponential coherence spectrum are employed to describe the inflow turbulence random field over the rotor plane, which is simulated using the computer program, TurbSim [8].

For the hydrodynamic loading on the support structure, irregular long-crested waves are simulated using a JONSWAP spectrum [9]. This same wave spectrum is used for simulating linear and nonlinear irregular waves. Hydrodynamic loads are computed using Morison's equation [10]; Wheeler stretching [10] is used to represent water particle kinematics and hydrodynamic loads up to the changing instantaneous sea surface.

Once the time histories of the wind inflow turbulence field and the sea surface elevation are generated, stochastic time-domain simulations of the turbine response are performed using the computer program, FAST. FAST employs a combined modal and multi-body dynamics formulation for analysis of any turbine model. It models the tower and blades as flexible bodies and uses the first two bending modes in each of the longitudinal and transverse directions. More details related to the modeling capabilities of FAST may be found in the User's Guide [5].

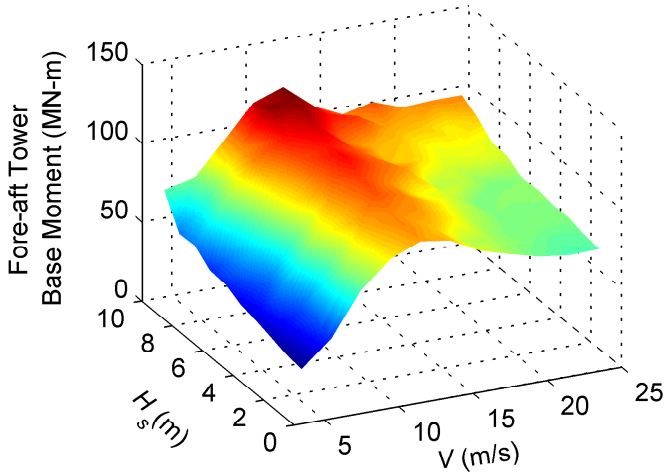

Figure 1. Variation with mean wind speed, V, and significant wave height, H_s, of the mean of the maximum values from six simulations of the fore-aft tower bending moment at mudline.

Table 1. Ten-minute statistics of the fore-aft tower bending moment (FATBM) at the mudline for different wind speed and wave height bins.

V	H_s	FATBM (MN-m)	
(m/s)	(m)	Max	SD
12.0	0.5	97.3	10.9
12.0	4.5	106.6	12.7
12.0	9.5	124.2	16.1
4.0	4.5	39.4	8.6
12.0	4.5	106.6	12.7
24.0	4.5	78.4	12.3

V: Mean wind speed; H_s, Significant wave height; Max: Ten-minute maximum; SD: Standard deviation.

Turbine Response

In order to derive statistics or distributions of turbine loads conditional on wind speed and wave height, multiple simulations have to be carried out for selected pairs of mean wind speed and significant wave height. Figure 1 shows the average of the ten-minute maximum fore-aft tower bending moment at mudline from six simulations for a range of (V, H_s) pairs. It is observed that this maximum load increases with wind speed, up to the rated wind speed of 11.5 m/s, and then decreases, as is expected, due to blade-pitch control actions. Waves also have

a clear influence on the turbine response; the maximum fore-aft tower bending moment increases almost linearly with wave height. Important statistics for representative wind speeds and wave heights are summarized in Table 1. It can be seen that while the maximum load drops considerably as the wind speed is increased above rated, the standard deviation of the load does not. As wave heights are increased, both the maximum and the standard deviation of the load increase. Based on the above observations, turbine long-term loads are expected to be governed by mean wind speeds near rated or by higher-than-rated wind speeds (where load variability may be larger) and by larger wave heights. Additional details related to specific turbine response statistics for different wind-wave combinations may be found in an earlier study by the authors [6].

Extrapolated Loads

In a previous study [6], we discussed the use of inverse FORM for the same 5 MW offshore turbine model as is used here, and we showed that long-term loads derived using inverse FORM are as accurate as those obtained by using the direct integration method. An additional advantage of using inverse FORM is that one can identify an environmental state (i.e., a (V, H_s) pair) that governs the extrapolated long-term target load of interest. This desired long-term load is the load level associated with a fractile, $p_3 = \Phi(u_3)$, which can in turn be mapped to the short-term distribution of the load extremes, conditional on the environmental state. Specifically, based on Eq. 2, the fractile, p_3, corresponding to the target reliability index, β, is obtained as follows:

$$p_3 = \Phi\left(\sqrt{\beta^2 - \left[\Phi^{-1}\left(F_V(v)\right)\right]^2 - \left[\Phi^{-1}\left(F_{H|V}(h)\right)\right]^2}\right) \qquad (3)$$

For the IEC Class I-B wind regime site (for which our turbine model is being considered), we assume that the ten-minute average wind speed, V, at hub height has a mean value of 10 m/s and that it can be described by a Rayleigh distribution. This distribution is truncated below the cut-in wind speed of 4 m/s and above the cut-out wind speed of 24 m/s, since we are interested only in studying turbine loads during operation. The significant wave height, H_s, conditional on the mean wind speed, is assumed to be represented by a two-parameter Weibull distribution. The expected value of H_s given V is based upon the JONSWAP correlation between wind speed and wave height [10], while the coefficient of variation for H_s given V is assumed to be constant at 0.2.

Load extremes required to establish the short-term distributions of the load given wind speed and wave height are extracted from time series of the turbine load as global maxima, i.e., as the largest load experienced in each ten-minute simulation. We have shown [6] that a mean wind speed of 16 m/s and a significant wave height of 5.5 m is the governing environmental state that causes the critical tower bending moment associated with a return period of 20 years. It was also shown that a large number of simulations are needed to obtain a stable short-term distribution for this environmental state and to estimate the p_3-quantile load, where p_3 is given by Eq. 3. An estimated conditional load distribution for the governing environmental conditions, obtained from 150 ten-minute simulations, is shown in Fig. 2. The exceedance probability in ten minutes, $(1 - p_3)$, corresponding to the desired load fractile, p_3, computed from Eq. 3, that is needed for a 20-year return period load is 3.87×10^{-6} while the maximum estimated exceedance fractile as obtained from the 150 simulations is several orders of magnitude higher at 6.60×10^{-3} $(= 1/151)$. Clearly, extrapolation to the desired rarer probability level is required. We obtain the desired 20-year load of 136.6 MN-m by fitting a two-parameter Weibull distribution to the tail of the empirical distribution data shown in Fig. 2. It was shown [6] that this predicted load based on inverse FORM is close to that predicted by direct integration.

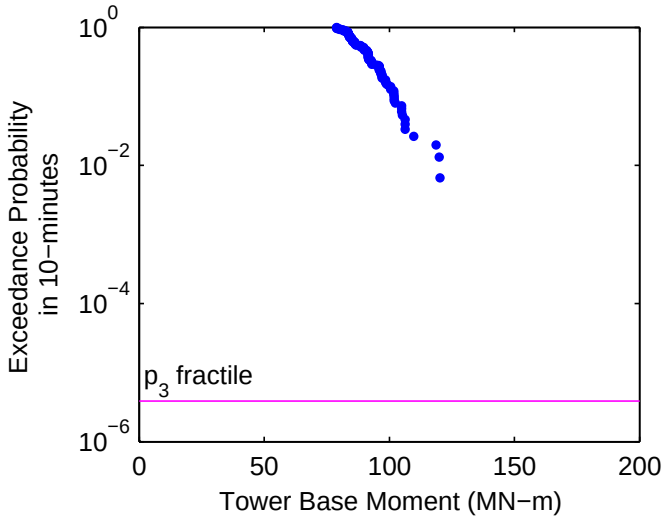

Figure 2. Empirical distribution of load (tower bending moment at mudline) extremes based on 150 simulations for a mean wind speed of 16 m/s and a significant wave height of 5.5 m.

Limitations

Long-term loads derived as presented above are based on simulation of irregular waves using a linear wave theory, which is not quite appropriate for waves in shallow waters that have higher crests and shallower troughs than are predicted by the linear wave theory. This wave asymmetry results in a non-zero skewness of the stochastic sea surface elevation process; a linear irregular wave process is Gaussian with zero skewness. The use of a nonlinear wave theory makes it possible to model this wave asymmetry; this is required for more accurate wave kinematics too. Water particle velocities and accelerations predicted by a linear wave theory are generally smaller than those predicted by a nonlinear wave theory. Ultimately, hydrodynamic loads predicted by linear wave kinematics can also be unconservative. For

these reasons, we seek to discuss next the influence of nonlinear waves on turbine tower loads.

SIMULATION OF NONLINEAR IRREGULAR WAVES

Linear wave theory for regular or irregular waves involves solution of Laplace's equation expressed in terms of a velocity potential and the use of linearized boundary conditions [10]. For nonlinear waves, the theory involves application of a perturbation approach to solve Laplace's equation with nonlinear boundary conditions. Sharma and Dean [1] used such an approach to derive a nonlinear wave theory for finite water depths. We will use the formulation of Sharma and Dean, which is described very briefly below. This theory has also been recommended in some guidelines for offshore structures [11].

Theory

The nonlinear sea surface elevation, $\eta(t)$, may be expressed as a sum of first- and second-order components, such that $\eta(t) = \eta_1(t) + \eta_2(t)$. The first-order component, $\eta_1(t)$, is expressed as in linear wave theory by

$$\eta_1(t) = \sum_{m=1}^{N} A_m \cos(\omega_m t - \phi_m) \tag{4}$$

where ω_m refers to the frequency of the m^{th} wave component and ϕ_m is the associated random phase assumed uniformly distributed over $[0, 2\pi]$. The amplitudes of the wave components, A_m, are Rayleigh distributed random variables whose mean square value is given as $E[A_m^2] = 2S(\omega_m)d\omega$ where $S(\omega_m)$ refers to the one-sided power spectral density function of the sea surface elevation process. The integer, m, in Eq. 4 refers to a frequency index that ranges from 1 to N, the total number of wave components represented in the simulated wave train.

The second-order component, $\eta_2(t)$, is obtained as a result of the interactions of sums and differences of frequencies as follows:

$$\eta_2(t) = \sum_{m=1}^{N}\sum_{n=1}^{N}\left[A_m A_n \left\{B_{mn}^{-}\cos(\psi_m - \psi_n) + B_{mn}^{+}\cos(\psi_m + \psi_n)\right\}\right] \tag{5}$$

where $\psi_m = (\omega_m t - \phi_m)$ and the second-order transfer functions, B_{mn}^{-} and B_{mn}^{+}, are obtained from solution of Laplace's equation for the velocity potential with nonlinear boundary conditions. They (i.e., B_{mn}^{-} and B_{mn}^{+}) are functions of frequency and wave number and are independent of the spectrum used.

The velocity potential, Φ, is comprised of first and second-order components such that $\Phi = \Phi_1 + \Phi_2$. These first and second-order velocity potentials are given as follows:

$$\Phi_1 = \sum_{m=1}^{N} b_m \frac{\cosh(k_m(h+z))}{\cosh(k_m h)} \sin\psi_m \tag{6}$$

$$\Phi_2^{=} \frac{1}{4}\sum_{m=1}^{N}\sum_{n=1}^{N}\left[b_m b_n \frac{\cosh(k_{mn}^{\pm}(h+z))}{\cosh(k_{mn}^{\pm}h)} \frac{D_{mn}^{\pm}}{(\omega_m \pm \omega_n)} \sin(\psi_m \pm \psi_n)\right] \tag{7}$$

where $b_m = A_m g/\omega_m$ and $k_{mn}^{\pm} = |k_m \pm k_n|$. Also, the linear dispersion relation, $\omega_m^2 = g k_m \tanh(k_m h)$, relates the wave number, k_m, to the frequency, ω_m, where h is the water depth and g is acceleration due to gravity. Expressions for the transfer functions, $B_{mn}^{\pm}$ and $D_{mn}^{\pm}$, appearing in Eqs. 5 and 7, respectively, are derived in [1] and also summarized in [12]. The horizontal water particle velocity, $u(z,t)$, and the horizontal water particle acceleration $\dot{u}(z,t)$ may be obtained from the velocity potential by taking derivatives such that $u(z,t) = \partial\Phi/\partial x$ and $\dot{u}(z,t) = \partial u(z,t)/\partial t$. Second-order waves are thus obtained as a result of sum and difference interactions between pairs of frequencies. The phases of the second-order contributions are also determined by sum and difference interactions of the phases of the first-order component phases, which are random.

Simulation of irregular (random) linear or first-order waves, which involves a single summation (Eq. 4), can be efficiently performed using the Inverse Fast Fourier Transform (IFFT). On the other hand, simulation of random nonlinear or second-order waves according to Eq. 5 involves a double summation, which can be more expensive. However, one can rewrite the double summation as a single summation by appropriately re-assembling and rewriting indices (or coefficients) in the double summation. Once the indices for an equivalent single summation are assembled, a one-dimensional IFFT procedure, similar to that for linear waves, can be used to perform the nonlinear wave simulations more efficiently.

Implementation in FAST

The nonlinear irregular wave model formulation discussed above has been incorporated into the computer program FAST, which performs coupled aeroelastic and hydrodynamic analysis of wind turbines. All of the following results are obtained from such FAST analyses, which consider the dynamic behavior of an offshore wind turbine with a focus on tower bending loads. For a study on the influence of nonlinear waves on a rigid stand-alone monopile, see Agarwal and Manuel [12].

LOADS ON THE TURBINE MONOPILE

To understand the effect of wave loads, we study hydrodynamic loads on the monopile support structure of the turbine. The monopile is a cylinder of 6 m diameter, and the water depth is 20 m. We compute water particle kinematics from linear and nonlinear irregular waves, while using Wheeler stretching to represent kinematics up to the instantaneous free surface. We use Morison's equation [10] to compute the hydrodynamic loads per unit length, f as follows:

$$f = f_D + f_M = \frac{1}{2}C_D \rho D u_r |u_r| + \frac{\pi D^2}{4} C_M \rho \dot{u}_r \tag{8}$$

where f_D and f_M are drag and inertia forces, respectively. Also, C_D is the drag coefficient taken as 1.0, C_M is the inertia coefficient taken as 2.0 [4], u_r is the relative horizontal velocity between water particles and the structure, $\dot{u}_r$ is the relative horizontal water particle acceleration, ρ is the density of water, and D is the diameter of the cylinder. The response of the tower as part of the overall turbine is computed from a dynamic analysis performed with the computer program, FAST.

Loads for the Governing Environmental State

When the linear theory for waves was used, a mean wind speed, V, of 16 m/s and a significant wave height, H_s, of 5.5 m was found to be the environmental state that governed the long-term tower bending moment for a return period of 20 years, as has been discussed earlier (see Fig. 2). We now investigate how much tower loads change when nonlinear irregular waves are employed, for these same environmental conditions.

Table 2 shows ten-minute maxima of the fore-aft tower bending moment (FATBM) computed using linear and nonlinear waves. When wind is not considered, loads from the nonlinear waves are about 17% larger than those due to linear waves, which indicates the importance of nonlinear waves. However, loads from linear and nonlinear waves are only slightly different when wind is included and the turbine is in operation. This is because for this (V, H_s) combination, loads due to waves alone make up only a small fraction (about one-fourth) of the loads due to both wind and waves. Based on this, we might say that 20-year loads may not differ greatly whether linear or nonlinear waves are used. However, the governing environmental state for long-term loads (computed using inverse FORM, for example) may itself change when the wave model is changed. It is therefore important that we study the influence of wave model choice on loads for other possible environmental states as well.

Table 2. Ten-minute maximum fore-aft tower bending moment (in MN-m) at the mudline, averaged over 20 simulations, computed with linear and nonlinear irregular waves using a JONSWAP spectrum with H_s = 5.5 m and T_p = 11.2 sec, and V = 16 m/s.

	Ten-minute maximum fore-aft tower bending moment at mudline (MN-m)	
	without wind	with wind
Linear waves	25.7	89.4
Nonlinear waves	29.9	90.9
Ratio	1.17	1.02

Loads for an Extreme Environmental State

We now consider environmental conditions involving a higher significant wave height of 7.5 m with a mean wind speed of 16 m/s. This combination of V and H_s lies on the so-called 20-year environmental contour obtained by setting $u_3 = 0$ in Eq. 2. The environmental contour method, which uses such combinations of environmental parameters to predict long-term loads (in this case, associated with a 20-year return period), assumes that the response is uncoupled from the environment and that computing the median response given the environmental parameters is sufficient to describe its variability (see [6] for more details). For the selected significant wave height, we assume a peak spectral period, T_p, of 12.3 sec, which corresponds to a wave steepness, $s = H_s/L_z$, of 0.06. Here, L_z is the wavelength corresponding to the zero-crossing period, T_z, based on the linear dispersion relation; also T_z is related to the peak spectral period, T_p, for a JONSWAP wave spectrum [11]. Nonlinear waves that result from use of the second-order model presented are assumed valid up to a steepness of around 0.08 [13]. Therefore, a steepness of 0.06 is a severe case of wave nonlinearity.

Table 3. Comparison of statistics of sea surface elevation process simulated using linear and nonlinear irregular wave model for a JONSWAP spectrum with H_s = 7.5 m and T_p = 12.3 sec.

Sea-surface elevation statistics	Wave model	
	linear	nonlinear
Std.Dev. (m)	1.8	2.0
Max (m)	5.6	6.6
Skewness	0.0	0.1
Kurtosis	2.9	3.2
Peak Factor*	3.0	3.3

* Median (over 50 simulations) ten-minute extreme peak factor.

Statistical moments, maximum values, and peak factors (averaged over 50 simulations, except for peak factors that are median values) of the sea surface elevation process, simulated using linear and nonlinear irregular waves, are summarized in Table 3. Statistical moments are computed from the simulated time series, and they match the target moments computed from a theoretical formulation presented by Langley [14]. Nonlinear waves have a non-zero skewness and a kurtosis larger than three, which indicates the non-Gaussian character of these nonlinear waves. Because of the larger skewness and kurtosis, and hence the somewhat larger peak factor, associated with nonlinear waves, extremes from nonlinear waves are larger than for linear waves. Since nonlinear waves tend to have sharper crests, the maximum of the sea surface elevation is larger (by about 1 m or 18%) than for linear waves. Due to these larger wave heights, it is expected that a greater portion of the monopile would get submerged and, as a result, the monopile would experience greater lateral base forces due to hydrodynamic loads. The loads are further amplified because particle velocities and accelerations are also larger for nonlinear waves (see [12]).

Table 4 shows statistics of the fore-aft tower bending moment (averaged over 50 ten-minute simulations). When wind is not included, the maximum load (with both drag and inertia

Table 4. Comparison of statistics, averaged over 50 simulations, of the fore-aft tower bending moment at the mudline for linear and nonlinear waves, for a JONSWAP spectrum with H_s = 7.5 m and T_p = 12.3 sec, and wind speed, V = 16 m/s.

	Fore-aft tower bending moment at mudline							
	without wind						with wind	
Hydrodynamics →	drag		inertia		total		total	
Wave model →	linear	nonlinear	linear	nonlinear	linear	nonlinear	linear	nonlinear
Mean (MN-m)	−1.2	−1.1	−1.5	−1.5	−1.1	−1.0	45.5	45.6
Max (MN-m)	13.9	26.2	31.2	43.6	35.4	53.8	97.1	107.5
Std.Dev. (MN-m)	2.2	3.4	9.8	12.1	10.0	12.7	13.3	14.0
Skewness	1.6	1.9	−0.1	−0.1	0.1	0.2	0.2	0.3
Kurtosis	10.5	13.4	3.3	3.7	3.4	4.0	3.4	4.0
Peak Factor (PF)*	6.3	7.3	3.3	3.5	3.6	4.0	3.8	4.1
PF-Gaussian **	3.2	3.3	3.1	3.2	3.1	3.2	3.4	3.4

* Median (over 50 simulations) ten-minute extreme peak factor.
** Peak factor computed from zero-crossing rate of the process assuming it were Gaussian.

forces accounted for) with the nonlinear waves is about 54 MN-m, which is about 52% larger than that due to linear waves. When winds are included, the maximum load with nonlinear waves is about 108 MN-m, only about 11% larger than that with linear waves—still a significant increase. Table 4 also shows that the mean value of the tower bending moment is close to zero with waves alone as input; this is because wave forces, in the absence of currents, are zero-mean processes, while wind-induced forces cause a non-zero mean that results from a non-zero mean longitudinal wind speed. To understand the influence of wave nonlinearity, we focus our attention on loads in the absence of winds, where it is also useful to study loads due to drag and inertia forces separately. Table 4 shows clearly that this monopile is dominated by inertia loads (see [12] for more details on why inertia loads dominate), as is typical for such large-diameter monopile cylinders in shallow waters. Loads due to inertia forces alone increase from about 31 MN-m (with linear waves) to 44 MN-m (with nonlinear waves) representing an increase of about 40%. On the other hand, loads due to drag forces alone increase from 14 MN-m (with linear waves) to about 26 MN-m (with nonlinear waves)—an increase of nearly 90%. Clearly, wave nonlinearity has a greater influence on drag forces. Note that the nonlinearity of waves increases both particle velocity and acceleration by similar amounts [12]; however, since drag forces are proportional to the square of the particle velocity and inertia forces are only linearly proportional to the particle acceleration (Eq. 8), the increase in loads due to wave nonlinearity is more significant for drag forces.

We can attempt to further understand hydrodynamic loads by studying the non-Gaussian character in these load processes. The degree to which a process is non-Gaussian relates to the extent by which its skewness deviates from zero and its kurtosis deviates from three. Using the mean-upcrossing rate of a random process, we can compute a theoretical peak factor for a specified exposure time assuming the process were Gaussian [15], and compare that to the actual peak factor computed directly and empirically from realizations of the process. A process with a positive skewness and a kurtosis greater than three (as is the case here) will generally lead to larger peak factors. This will, in turn, result in larger extremes associated with any specified rare probability level compared to those predicted for a Gaussian process. Note that it is such low exceedance probability levels that are of eventual interest in predicting long-term loads for ultimate limit states. Table 4 shows that skewness, kurtosis and peak factor estimates from the simulations are always larger with nonlinear waves. As a result, extreme loads predicted based on the use of nonlinear waves will also be larger. Furthermore, deviations from the Gaussian are greater for drag forces and, therefore, the influence of nonlinear waves on loads would be even more pronounced for a structure that is dominated by drag forces—e.g., for slender members such as those in a jacket structure.

To further investigate the influence of wave nonlinearity, we study a representative 200-second segment from a single ten-minute simulation time history. Figure 3 shows that crests of the sea surface elevation process are systematically higher for the nonlinear wave model than for the linear model. Consequently, positive maxima of the tower base shear and bending moment at the mudline are also larger for nonlinear waves, when winds are not included as shown in Fig. 4. The power spectrum of the sea surface elevation (Fig. 3) for the nonlinear case shows a secondary peak at about 0.16 Hz, which is twice the spectral peak frequency of 0.08 Hz (since T_p = 12.3 sec), and a small peak close to a zero frequency. Such secondary peaks arise due to sum and difference interactions of frequencies according to the second-order nonlinear wave model (see Eq. 5). These secondary peaks also appear in power spectra of both the tower base shear and the tower bending moment (Fig. 4). The tower bending moment power spectrum has a significant peak at around 0.27 Hz, which is the natural frequency for the first bending mode of vibration of the tower in the fore-aft direction. This clearly suggests that

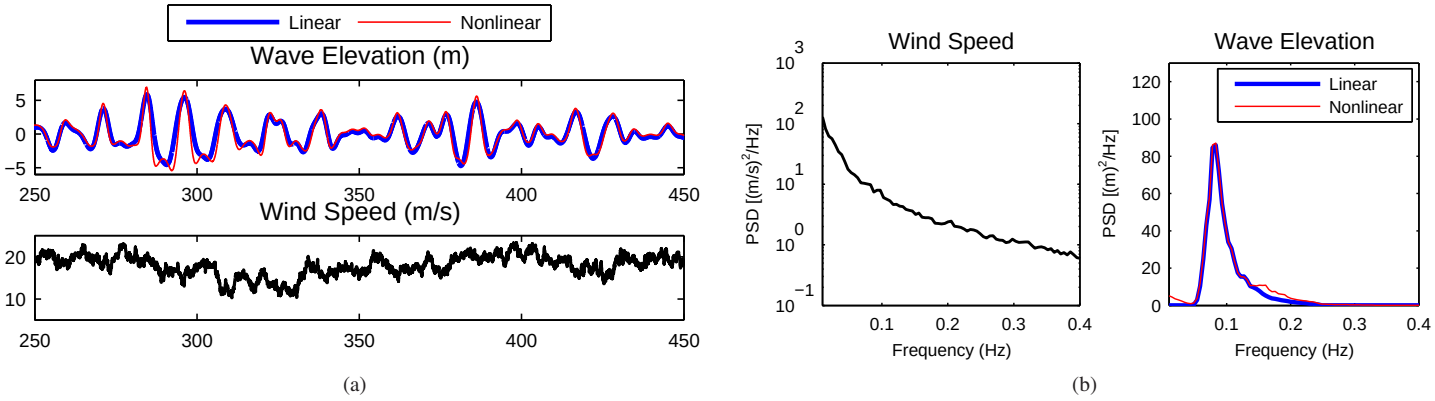

Figure 3. (a) Time series and (b) power spectral density (PSD) functions of wind speed for V = 16 m/s and of wave elevation for linear and nonlinear waves simulated using a JONSWAP spectrum with H_s = 7.5 m and T_p = 12.3 sec.

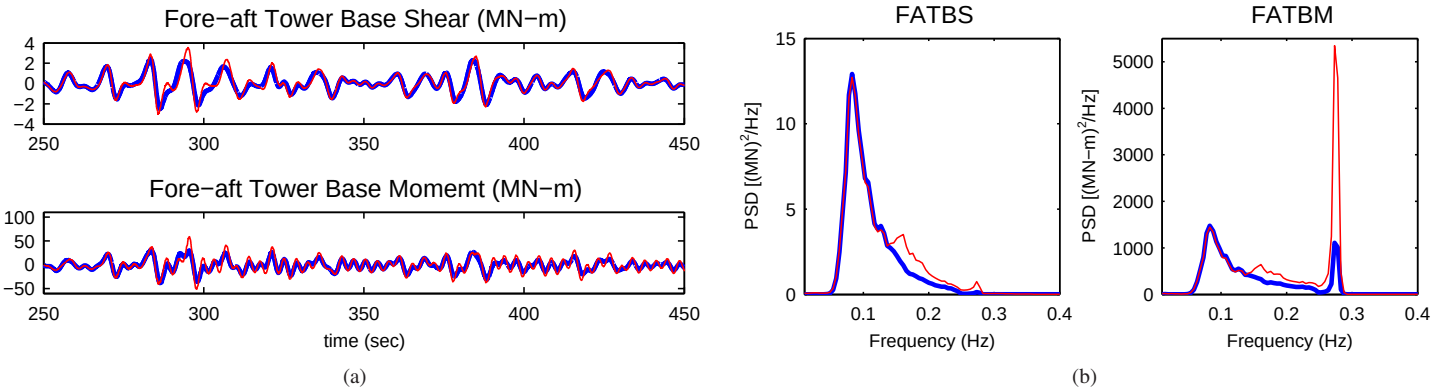

Figure 4. (a) Time series and (b) power spectral density (PSD) functions of fore-aft tower base shear (FATBS) and tower bending moment (FATBM) at the mudline for H_s = 7.5 m and T_p = 12.3 sec, when wind is not included.

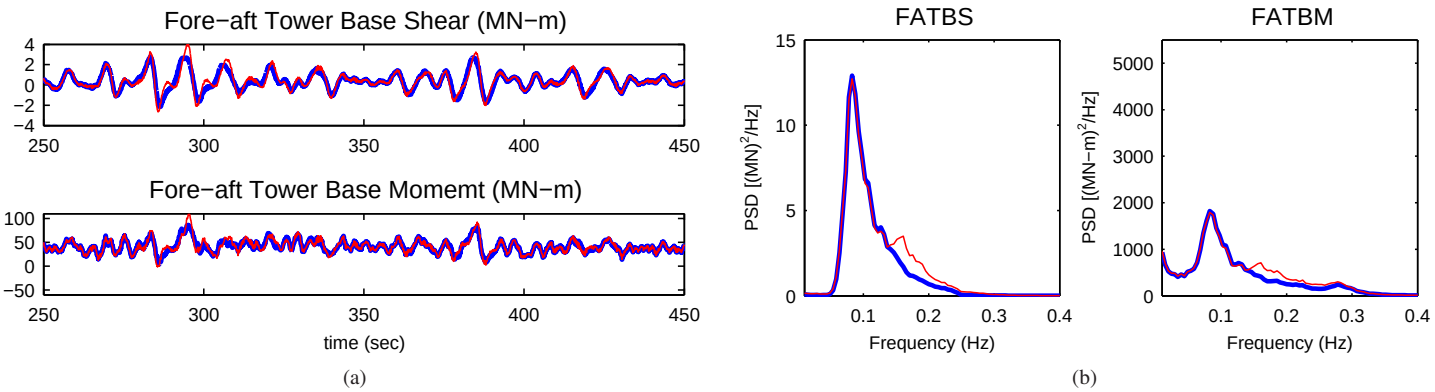

Figure 5. (a) Time series and (b) power spectral density (PSD) functions of fore-aft tower base shear (FATBS) and tower bending moment (FATBM) at the mudline for V = 16 m/s, H_s = 7.5 m and T_p = 12.3 sec, when wind is included.

tower dynamics may be important in the overall response. The response of the turbine tower when winds are included is shown in Fig. 5. The influence of winds on the tower base bending moment is more pronounced than on the tower base shear, because of the large lever arm associated with the moment due to wind forces at the level of the rotor plane. Comparing time series of the tower bending moment when winds are included (Fig. 5) to when winds are not included (Fig. 4), we see that winds add a mean component to the tower bending moment. The turbulent character of the wind is also evident. More interesting is the observation that the peak at the tower natural frequency in the power spectrum of the tower bending moment has almost disappeared when winds are included. Such behavior has also been reported by other researchers [16, 17]; it is due to aerodynamic damping from wind loads when the turbine is in operation, which we briefly discuss next.

Tarp-Johansen and Frandsen [18] developed a simple linear single-degree-of-freedom (SDOF) model to describe wind turbine dynamics. Their model considers hydrodynamic forces due to inertia only (in the present study, too, inertia forces dominate) and assumes the rotor to be a bluff body, while including the effect of aerodynamic loads on the rotating blades. Damping is assumed to be the sum of structural and aerodynamic damping. The aerodynamic damping coefficent is expressed as $c_{rot} = \rho_A C_T V A$, where ρ_A is the density of air, V is the mean wind speed at hub height, A is the swept area of the rotor, and C_T is the thrust coefficient. Using the properties and dimensions of the 5 MW turbine model under study here, the aerodynamic damping ratio (as a fraction of critical damping) is estimated to be 7%, while the structural damping ratio is assumed to be 1%. For the sake of comparison, we estimate the damping ratio from power spectra of the simulated tower response (in Figs. 4 and 5) using the half-power bandwidth method; then, the damping ratios with and without winds are found to be about 3% and 9%, respectively. From this, the aerodynamic damping ratio is estimated to be about 6%, which reasonably well matches the aerodynamic damping ratio from the simple SDOF model [18]. The relatively large damping in the presence of wind loads compared to the lighter damping when winds are not included explains why the first vibration mode of tower bending is greatly damped out when winds are present.

LONG-TERM ULTIMATE LOADS

Our interest is in predicting extreme loads associated with rare (low) probability of exceedance levels. Earlier, with linear irregular waves, we discussed the subject of statistical extrapolation of wind turbine loads in some detail, and derived long-term loads for our 5MW wind turbine model for a return period of 20 years. We are interested in performing similar calculations for turbine loads using nonlinear waves. Such calculations would, in principle, require multiple simulations of the turbine response for various possible (V, H_s) combinations, followed by estimation of short-term distributions of load conditional on environment and, finally, use of the direct integration method or inverse FORM to predict long-term loads for the desired return period. In the present study, we have not undertaken this entire exercise; rather we have focused on understanding the mechanics of nonlinear waves and their influence on turbine loads for two (V, H_s) pairs. For V = 16 m/s and H_s = 5.5 m, which was the governing environmental state for long-term tower loads with linear waves, we have shown (Table 2) that nonlinear waves do not result in significantly larger loads than those due to linear waves. However, the governing environmental conditions are likely to be different with nonlinear waves. Hence, we have compared loads based on linear and nonlinear waves in an extreme environmental state—V = 16 m/s and H_s = 7.5 m (Table 4). For this extreme state, Fig. 6 shows short-term probability distributions of ten-minute load maxima when linear and nonlinear waves are used. The distributions of load maxima for the two cases are strikingly different. Any rare load predicted by statistical extrapolation for the nonlinear wave model would be significantly larger than one predicted for linear waves. This observation is also consistent with our earlier discussion (in Table 4) about large non-Gaussian skewness, kurtosis, and peak factor values for nonlinear waves, which are responsible for the larger rare (low-probability) loads compared to when linear waves are modeled. From Fig. 6, we might note that the largest simulated tower bending moment at the mudline (associated with an exceedance probability in ten minutes of 1/51 or 0.0196) with the linear waves is 126.5 MN-m, while that with the nonlinear waves is 184.3 MN-m, about 46% higher. In an analysis based on inverse FORM using environmental contours [3], only the median extreme load would be required for this extreme state; for nonlinear waves, this load is about 8% larger than that due to linear waves (based on 50 simulations). On the basis of the results presented, for environmental states associated with long return periods, we expect that tower loads due to nonlinear waves will likely be somewhat larger than those due to linear waves. Accordingly, we believe that it is important that in estimating long-term loads for an offshore wind turbine sited in shallow water depths, nonlinear irregular waves are modeled.

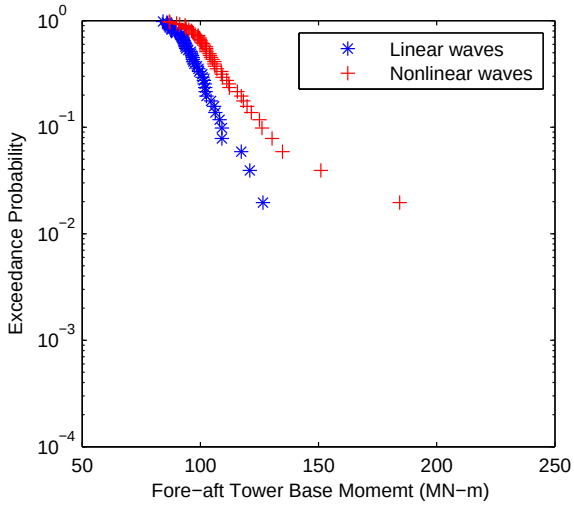

Figure 6. Empirical probability distributions of ten-minute maxima of the fore-aft tower bending moment at the mudline based on 50 ten-minute simulations with V = 16 m/s, H_s = 7.5 m and T_p = 12.3 sec.

SUMMARY AND CONCLUSIONS

Our objective in this study was to investigate long-term loads for a utility-scale 5MW offshore wind turbine sited in 20 meters of water. Our focus was on the fore-aft tower bending moment at the mudline. We presented the theory for modeling nonlinear (second-order) irregular waves, which is more appropriate than the use of linear waves for shallow water depths, and have incorporated this nonlinear wave model in a time-domain simulator that performs aero-servo-hydro-elastic analysis of wind turbines.

We have studied the influence of modeling nonlinear waves on loads for a monopile support structure (a cylinder of 6 m diameter) of the turbine and compared the loads to those based on more conventional linear wave theory.

We used the inverse first-order reliability method to derive the extreme tower bending moment for a 20-year return period for the 5MW turbine, when linear irregular waves were used. The governing environmental state (mean wind speed and significant wave height) important for this 20-year load was also derived. For this governing mean wind speed of 16 m/s and significant wave height of 5.5 m, we investigated tower loads when nonlinear irregular waves were used. We found that while loads due to waves alone are larger when nonlinear waves are modeled (compared to modeling of linear waves), the difference disappears when wind is also included as wind load effects dominate waves for this environmental state. We investigated the effect of wave nonlinearity on tower loads in more detail for an extreme environmental state (mean wind speed of 16 m/s and significant wave height of 7.5 m). It was found that loads due to nonlinear waves could be significantly larger than those from linear waves especially for drag-dominated support structures. Based on simulations, we also estimated empirical short-term distributions of the fore-aft tower bending moment at the mudline due to linear and nonlinear irregular waves; it was seen that, with nonlinear waves, loads corresponding to rare fractile levels are significantly larger than those predicted with linear waves.

In summary, findings from this study suggest that nonlinear irregular waves can have an important influence on the hydrodynamic loads experienced by an offshore wind turbine support structure. Therefore, it is important that nonlinear waves be considered when predicting long-term loads in evaluating limit states for offshore wind turbine design.

ACKNOWLEDGMENT

The authors gratefully acknowledge the financial support provided by CAREER Award No. CMMI-0449128 and Award No. CMMI-0727989 from the National Science Foundation. They also acknowledge assistance from Dr. Jason Jonkman at the National Renewable Energy Laboratory with the wind turbine simulation model used in this study.

REFERENCES

[1] Sharma, J. N., and Dean, R. G., 1979. Development and Evaluation of a Procedure for Simulating a Random Directional Second-order Sea Surface and Associated Wave Forces. Tech. Rep. Ocean Engineering Report No. 20, University of Delaware, Newark, DE.

[2] IEC-61400-3, 2005. *Wind Turbines - Part 3: Design Requirements for Offshore Wind Turbines*. International Electrotechnical Commission, TC88 WG3 Committee Draft.

[3] Saranyasoontorn, K., and Manuel, L., 2006. "Design Loads for Wind Turbines using the Environmental Contour Method". *Journal of Solar Energy Engineering, Transactions of the ASME,* **128**(4), pp. 554–561.

[4] Jonkman, J. M., Butterfield, S., Musial, W., and Scott, G., 2007 (to be published). Definition of a 5-MW Reference Wind Turbine for Offshore System Development. Tech. Rep. NREL/TP-500-38060, National Renewable Energy Laboratory, Golden, CO.

[5] Jonkman, J. M., and Buhl Jr., M. L., 2005. FAST User's Guide. Tech. Rep. NREL/EL-500-38230, National Renewable Energy Laboratory, Golden, CO.

[6] Agarwal, P., and Manuel, L., 2007. "Simulation of Offshore Wind Turbine Response for Extreme Limit States". In 26th International Conference on Offshore Mechanics and Arctic Engineering, OMAE2007.

[7] Winterstein, S. R., Ude, T. C., Cornell, C. A., Bjerager, P., and Haver, S., 1993. "Environmental Contours for Extreme Response: Inverse FORM with Omission Factors". In Proceedings, ICOSSAR-93.

[8] Jonkman, B. J., and Buhl Jr., M. L., 2007. TurbSim User's Guide. Tech. Rep. NREL/TP-500-41136, National Renewable Energy Laboratory, Golden, CO.

[9] DNV-OS-J101, 2007. *Design of Offshore Wind Turbine Structures, Offshore Standard*. Det Norske Veritas.

[10] Barltrop, N., and Adams, A., 1991. *Dynamics of Fixed Marine Structures*. Butterworth-Heinemann, London.

[11] DNV-RP-C205, 2007. *Environmental Conditions and Environmental Loads, Recommended Practice*. Det Norske Veritas.

[12] Agarwal, P., and Manuel, L., 2008. "Wave Models for Offshore Wind Turbines". In ASME Wind Energy Symposium, AIAA.

[13] Hu, S.-L. J., and Zhao, D., 1993. "Non-Gaussian Properties of Second-order Random Waves". *Journal of Engineering Mechanics,* **119**(2), pp. 344–364.

[14] Langley, R., 1987. "A Statistical Analysis of Nonlinear Random Waves". *Ocean Engineering,* **14**(5), pp. 389–407.

[15] Madsen, H. O., Krenk, S., and Lind, N. C., 1986. *Methods of Structural Safety*. Prantice Hall, Englewood Cliffs, NJ.

[16] Jonkman, J., Butterfield, S. P., Passon, P., Larsen, T., Camp, T., Nichols, J., Azcona, J., and Martinez, A., 2008. Offshore Code Comparison Collaboration within IEA Wind Annex XXIII: Phase II Results Regarding Monopile Foundation Modeling. Tech. Rep. NREL/CP-500-42471, National Renewable Energy Laboratory, Golden, CO.

[17] Tempel, J., and Molenaar, D.-P., 2002. "Wind Turbine Structural Dynamics - A Review of the Principles for Modern Power Generation, Onshore and Offshore". *Wind Engineering,* **26**(4), pp. 211–220.

[18] Tarp-Johansen, N. J., and Frandsen, S., 1999. A Simple Model for Offshore Wind Turbine Foundation Design. Tech. Rep. Design Regulations for Offshore Wind Turbines Project Document, Risoe National Laboratory, Denmark.